Frequency Encoding in the Presence of Extreme Static Field Gradients

K. M. Koch[1], K. F. King[1], W. Chen[2], G. Gold[3], and B. A. Hargreaves[3]

[1]Global Applied Science Laboratory, GE Healthcare, Waukesha, WI, United States, [2]Global Applied Science Laboratory, GE Healthcare, Menlo Park, CA, United States, [3]Department of Radiology, Stanford University, Stanford, CA, United States

Introduction:

3D Multi-Spectral-Imaging (MSI) imaging techniques can significantly reduce susceptibility artifacts near embedded metallic devices at both 1.5 and 3.0 Tesla [1,2,3]. Current incarnations of 3D-MSI are the MAVRIC [1], SEMAC [2], and VS-MSI [3] approaches. To date, the issues of requisite spectral coverage and frequency encoding limitations have seen little treatment in the context of imaging near metal. As 3D-MSI techniques become more commonly used in the clinical arena, an improved understanding of these considerations is desirable.

The top row in Figure 1 presents high-bandwidth (+/-125 kHz) 2D-FSE, SEMAC, and MAVRIC (both sum-of-squares spectral combination) images near a pair of stainless steel screws embedded in a human knee. While compared to 2D-FSE, SEMAC and MAVRIC are both able to dramatically improve the image quality in the vicinity of these screws, it is also apparent that there is remaining signal dropout directly adjacent to the screws (characterized by the distinct dipole dropout pattern). It is important to note that MAVRIC and SEMAC apply differing spectral and encoding strategies, which accounts for the slight difference in dropout and pileup artifacts. The crucial observation is that both cases are missing signal that drops out at similar spatial locations. The fate of this missing signal is the subject of this investigation.

Methods:

It has previously been shown that the MAVRIC and VS-MSI approaches possess spectral information that can be used to construct field maps near metal devices [3]. A MAVRIC-based field map is displayed in Figure 1. Using this map, we can estimate the local gradient in the (S/I) readout direction, Gx, which is plotted as a ratio of the applied frequency-encoding gradient, Gr.

An orange line in the MAVRIC image indicates a segmented profile chosen for further analysis. The sum-of-squares composite intensity and as well as a selection of spectral bin intensities are plotted in the left panel. An important feature of this plot is that the sum of the spectral bin intensities is decreasing as the metal interface is approached.

To further explore this signal reduction, the lower right panel of Figure 1 shows plots of the local induction gradient and the sum-of-squares intensity. The gradient is plotted only where sufficient signal is available for field map estimation. It can be seen that the signal begins to rapidly decay as the gradient approaches and supersedes a value equal to the frequency encoding gradient (or where the net local gradient is twice the applied gradient). On the other side of the metal, we can see that the signal remains low until the gradient has risen to a value that is nearly equal and opposite to the encoding gradient. In this case, we begin to see pileup artifacts.

Bloch simulations of MAVRIC spectral bins were also performed in the presence of a similar implant. Predictions of the spin dephasing and pileup effects were enabled by effectively simulating 80 spins per encoded pixel. The simulated signal trends (Figure 2) are clearly similar to the measured data. In the simulated case, spectral bins nearly 40 kHz off-resonance were included in the composite image – though it is clear that the signal in these bins is dramatically reduced.

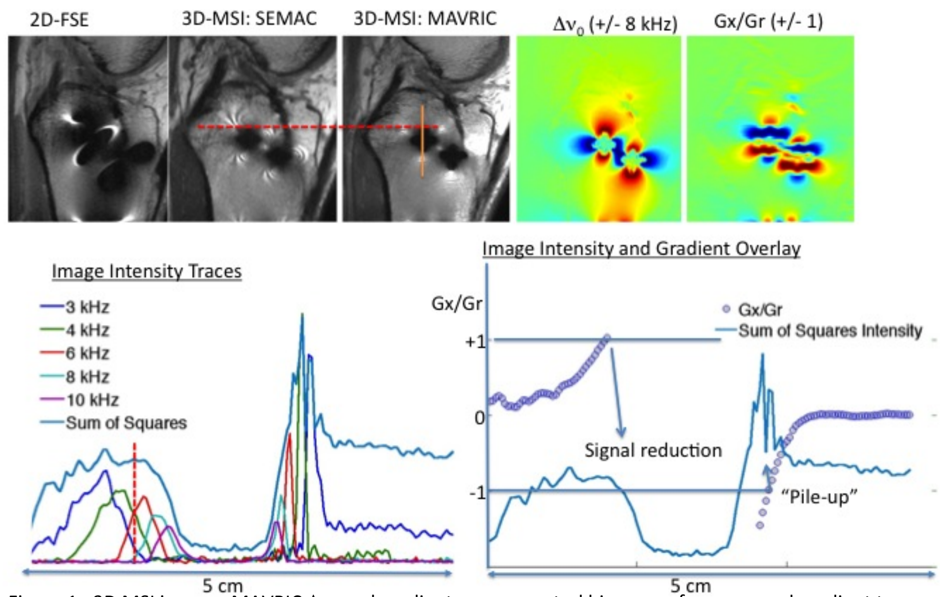

Figure 1: 3D MSI images, MAVRIC $\Delta\nu_0$ and gradient maps, spectral bin, sum of squares and gradient traces

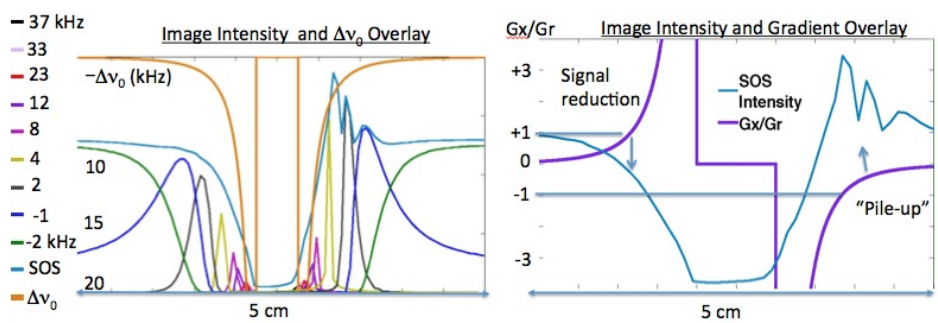

Figure 2: Simulated $\Delta\nu_0$ distribution and MAVRIC signal for a 1cm diameter stainless steel sphere at 1.5T.

Discussion:

This analysis demonstrates a few important principles. First, in regions where the local induced gradients exactly cancel the readout gradient, effective encoding resolution is degraded. This results in the "pile-up" condition. In these regions, the signal amplitude can be corrected via Jacobian multiplier methods -- but the resolution cannot be regained.

On the other hand, in locations where the local gradients are strongly supporting or overwhelmingly opposing the frequency-encode gradient, the observed signal loss cannot be regained. This lost signal results from the finite temporal resolution of acquired data (i.e. limited reception sampling/bandwidth) in conjunction with the strong gradients that alter the effective frequency-encoded resolution. When the effective resolution becomes greater than that determined by the applied frequency encode gradient and sampling bandwidth, phase cancelation of the imaged spin ensemble occurs -- which cannot be recovered under finite sampling (or reception bandwidth) conditions.

This signal reduction regime is found roughly where the local gradient magnitude surpasses the magnitude of the encoding gradient. As seen in both the experimental and simulated data, locations resonating beyond roughly 10 kHz suffer from these signal reduction effects. The size and shape of ensuing signal voids vary depending on implant geometry and composition. Often, when imaging near a larger implant, these voids will manifest as small, symmetric notches in the implant interface. While 3D-MSI techniques can substantially reduce artifacts near metal implants, the effects presented here are to be an expected artifact inherent to any method that relies on frequency encoding principles.

[1] Koch et al,MRM,61,2009,381-390, [2] Lu et al,MRM,62,2009,66-76 , [3] Koch et al, MRM, EarlyView, 2010, DOI: 10.1002/mrm.22523